1.7
ELECTRONIC SCALE

James R. Chelikowsky
University of Minnesota, Minneapolis, MN, USA

1. Real-space methods for *ab initio* calculations

Major computational advances in predicting the electronic and structural properties of matter come from two sources: improved performance of hardware and the creation of new algorithms, i.e., software. Improved hardware follows technical advances in computer design and electronic components. Such advances are frequently characterized by Moore's Law, which states that computer power will double every 2 years or so. This law has held true for the past 20 or 30 years and most workers expect it to hold for the next decade, suggesting that such technical advances can be predicted.

In clear contrast, the creation of new high performance algorithms defies characterization by a similar law as creativity is clearly not a predictable activity. Nonetheless, over the past half century, most advances in the theory of the electronic structure of matter have been made with new algorithms as opposed to better hardware. One may reasonably expect these advances to continue. Physical concepts such as the pseudopotentials and density functional theories coupled with numerical methods such as iterative diagonalization methods have permitted very large systems to be examined, much larger systems than could be handled solely by the increase allowed by computational hardware advances. Systems with hundreds, if not thousands, of atoms can now be examined, whereas methods of a generation ago might handle only tens of atoms.

The development of *real-space methods* for the electronic structure over the past ten years is a notable advance in high performance algorithms for solving the electronic structure problem. Real-space methods do not require an explicit basis. The convergence of the method, assuming a uniform grid, can be tested by varying only one parameter: the grid spacing. The method can be easily be applied to neutral or charged systems, to extended or localized systems, and to diverse materials such as simple metals, semiconductors,

S. Yip (ed.),
Handbook of Materials Modeling, 121–135.

and transition metals. These methods are also well suited for highly parallel computing platforms as few global communications are required. Review articles on these approaches can be found in Refs. [1–3].

2. The Electronic Structure Problem

Most contemporary descriptions of the electronic structure problem for large systems cast the problem within density functional theory [4]. The many body problem is mapped onto a one electron Schrödinger equation called the Kohn–Sham equation [5]. For an atom, this equation can be written as

$$\left(\frac{-\hbar^2 \nabla^2}{2m} - \frac{Ze^2}{r} + V_{\mathrm{H}}(\vec{r}) + V_{\mathrm{xc}}[\vec{r}, \rho(\vec{r})] \right) \psi_n(\vec{r}) = E_n \psi_n(\vec{r}) \tag{1}$$

where there are Z electrons in the atom, V_{H} is the Hartree or Coulomb potential, and V_{xc} is the exchange-correlation potential. The Hartree and exchange-correlation potentials can be determined from the electronic charge density. The eigenvalue and eigenfunctions, $(E_n, \psi_n(\vec{r}))$, can be used to determine the total electronic energy of the atom. The density is given by

$$\rho(\vec{r}) = -e \sum_{n,\mathrm{occup}} |\psi_n(\vec{r})|^2 \tag{2}$$

The summation is over all occupied states. The Hartree potential is then determined by

$$\nabla^2 V_{\mathrm{H}}(\vec{r}) = -4\pi e \rho(\vec{r}) \tag{3}$$

This term can be interpreted as the electrostatic interaction of an electron with the charge density of system.

The exchange-correlation potential is more problematic. Within density functional theory, one can define an exchange correlation potential as a functional of the charge density. The central tenant of the local density approximation [5] is that the total exchange-correlation energy may be written as

$$E_{\mathrm{xc}}[\rho] = \int \rho(\vec{r})\, \epsilon_{\mathrm{xc}}(\rho(\vec{r}))\, d^3r \tag{4}$$

where ϵ_{xc} is the exchange-correlation energy density. If one has knowledge of the exchange-correlation energy density, one can extract the potential and total electronic energy of the system. As a first approximation the exchange-correlation energy density can be extracted from a homogeneous electron gas. It is common practice to separate exchange and correlation contributions to ϵ_{xc}: $\epsilon_{\mathrm{xc}} = \epsilon_{\mathrm{x}} + \epsilon_{\mathrm{c}}$ [4].

It is not difficult to solve the Kohn–Sham equation (Eq. 1) for an atom. The potential, and charge density, is assumed to be spherically symmetric

and the Kohn–Sham problem reduces to solving a one-dimensional problem. The Hartree and exchange-correlation potentials can be iterated to form a self-consistent field. Usually the process is so quick for an atom that it can be done on desktop or laptop computer in a matter of seconds.

In three dimensions, as for a complex atomic cluster, liquid or crystal, the problem is highly nontrivial. One major difficulty is the range of length scales involved. For example, in the case of a multielectron atom, the most tightly bound, core electrons can be confined to within $\sim$0.1 Å whereas the outer valence electrons may extend over $\sim$1–5 Å. In addition, the nodal structure of the atomic wave functions are difficult to replicate with a simple basis, especially the cusp in a wave function at the nuclear site where the Coulomb potential diverges.

One approach to this problem is to form a basis combining highly localized functions with extended functions. This approach enormously complicates the electronic structure problem as valence and core states are treated on equal footing whereas such states are not equivalent in terms of their chemical activity.

Consider the physical content of the periodic table, i.e., arranging the elements into columns with similar chemical properties. The Group IV elements such as C, Si, and Ge have similar properties because they share an outer s^2p^2 configuration. This chemical similarity of the valence electrons is recognized by the *pseudopotential* approximation [6, 7].

The pseudopotential replaces the "all electron" potential by one that reproduces only the chemically active, or valence electrons. Usually, the pseudopotential subsumes the nuclear potential with those of the core electrons to generate an "ion core potential." As an example, consider a sodium atom whose core electron configuration is $1s^2 2s^2 2p^6$ and valence electron configuration is $3s^1$. The charge on the ion core pseudopotential is $+1$ (the nuclear charge minus the number of core electrons). Such a pseudopotential will bind only one electrons. The length scale of the pseudopotential is now set by the valence electrons alone. This permits a great simplification of the Kohn–Sham problem in terms of choosing a basis.

For the purposes of designing an *ab initio* pseudopotential let us consider a sodium atom. By solving for the Na atom, we know the eigenvalue, ϵ_{3s}, and the corresponding wave function, $\psi_{3s}(r)$ for the valence electron. We demand several conditions for the Na pseudopotential: (1) The potential bind only the valence electron, the 3s-electron for the case at hand. (2) The eigenvalue of the corresponding valence electron be identical to the full potential eigenvalue. The full potential is also called the *all-electron* potential. (3) The wave function be nodeless and *identical* to the "all electron" wave function outside the core region. For example, we construct a pseudo-wave function, $\phi_{3s}(r)$ such that $\phi_{3s}(r)=\psi_{3s}(r)$ for $r > r_c$ where r_c defines the size spanned by the *ion core*, i.e., the nucleus and core electrons. For Na, this means the "size" of $1s^2 2s^2 2p^6$

states. Typically, the core is taken to be less than the distance corresponding to the maximum of the valence wave function, but greater than the distance of the outermost node.

If the eigenvalue, $\epsilon_{\rm p}$, and the wave function, $\phi_{\rm p}(r)$, are known from solving the atom, it is possible to invert the Kohn–Sham equation to yield an *ion core* pseudopotential, i.e., a pseudopotential that when screened will yield the exact eigenvalue and wave function by construction:

$$V^{\rm p}_{\rm ion}(r) = \epsilon_p + \frac{\hbar^2\nabla^2\phi_{\rm p}}{2m\phi_{\rm p}} - V_{\rm H}(r) - V_{\rm xc}[r, \rho(r)] \tag{5}$$

Within this construction, the pseudo-wave function, $\phi_{\rm p}(r)$, should be identical to the all electron wave function, $\psi_{\rm AE}(r)$, outside the core: $\phi_{\rm p}(r) = \psi_{\rm AE}(r)$ for $r > r_{\rm c}$ will guarantee that the pseudo-wave function will yield similar chemical properties as the all electron wave function.

For $r < r_{\rm c}$, one may alter the all-electron wave function as one wishes, within certain limitations, and retain the chemical accuracy of the problem. For computational simplicity, we take the wave function in this region to be smooth and nodeless. Another very important criterion is mandated. Namely, the integral of the pseudocharge density, i.e., square of the wave function $|\phi_{\rm p}(r)|^2$, within the core should be equal to the integral of the all-electron charge density. Without this condition, the pseudo-wave function can differ by a scaling factor from the all-electron wave function, that is, $\phi_{\rm p}(r) = C \times \psi_{\rm AE}(r)$ for $r > r_{\rm c}$ where the constant, C, may differ from unity. Since we expect the chemical bonding of an atom to be highly dependent on the tails of the valence wave functions, it is imperative that the normalized pseudo wave function be identical to the all-electron wave functions. The criterion by which one insures $C = 1$ is called *norm conserving* [2].

An example of a pseudopotential, in this case the Na pseudopotential, is presented in Fig. 1. The ion core pseudopotential is dependent on the angular momentum component of the wave function. This is apparent from Eq. (5) where the $V^{\rm p}_{\rm ion}$ is "state dependent" or nonlocal. This nonlocal behavior is pronounced for first row elements, which lack p-states in the core, and for first row transition metals, which lack d-states in the core. A physical explanation for this behavior can be traced to the orthogonality requirement of the valence wave functions to the core states. This may be illustrated by considering the carbon atom. The 2s of carbon is orthogonal to the 1s state, whereas the 2p state is not required to be orthogonal to a 1p state. As such, the 2s state has a node; the 2p does not. In transforming these states to nodeless pseudo-wave functions, more kinetic energy associated with the 2s exists compared to the 2p state. The additional kinetic energy cancels the strong coulombic potential better for the 2s state than the 2p. In terms of the ion core pseudopotential, the 2s potential is weaker than the 2p state.

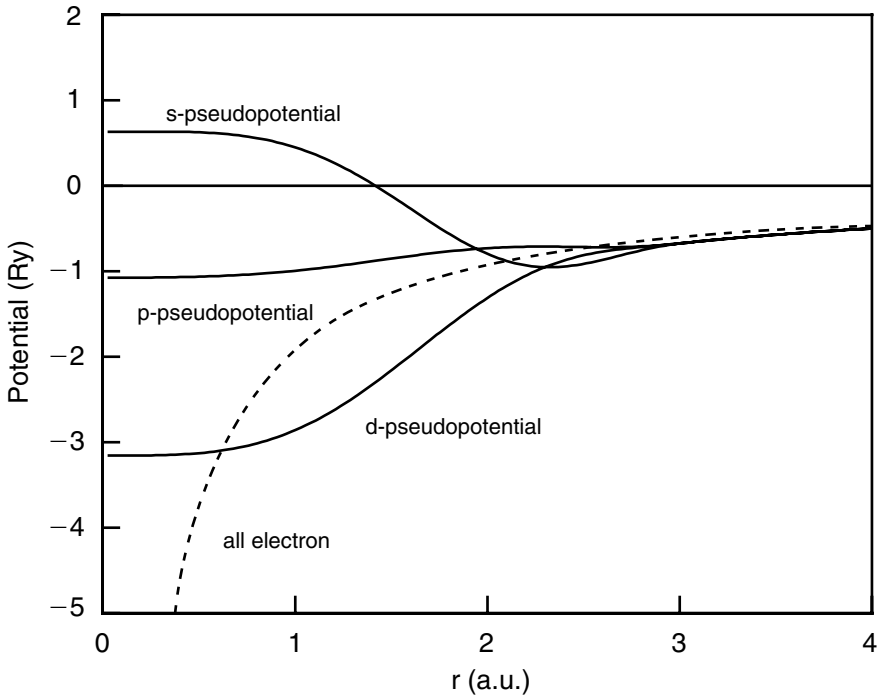

Figure 1. Pseudopotential compared to the all-electron potential for the sodium atom. This pseudopotential was constructed using the method of Troullier and Martins [8].

In the case of sodium, only three significant components (s, p, and d) are required for an accurate pseudopotential. Note how the d component is the strongest following the argument that no core states of similar angular momentum exist within the Na core. For more complex systems such as a rare earth metals, one might have four or more components. In Fig. 2, the 3s state for the all electron potential is illustrated. It is compared to the lowest s-state for the pseudopotential illustrated in Fig. 1

The Kohn–Sham equation can be rewritten for a pseudopotential as

$$\left(\frac{-\hbar^2 \nabla^2}{2m} + V_{\text{ion}}^{\text{p}}(\vec{r}) + V_{\text{H}}(\vec{r}) + V_{\text{xc}}[\vec{r}, \rho(\vec{r})] \right) \psi_n(\vec{r}) = E_n \psi_n(\vec{r}) \tag{6}$$

where $V_{\text{ion}}^{\text{p}}$ can be expressed as

$$V_{\text{ion}}^{\text{p}}(\vec{r}) = \sum_i V_{i,\text{ion}}^{\text{p}}(\vec{r} - \vec{R}_i) \tag{7}$$

where $V_{i,\text{ion}}^{\text{p}}$ is the ionic pseudopotential for the ith-atomic species located at position, $\vec{R}_i$. The charge density in Eq. (7) corresponds to a sum over the wave functions for occupied valence states.

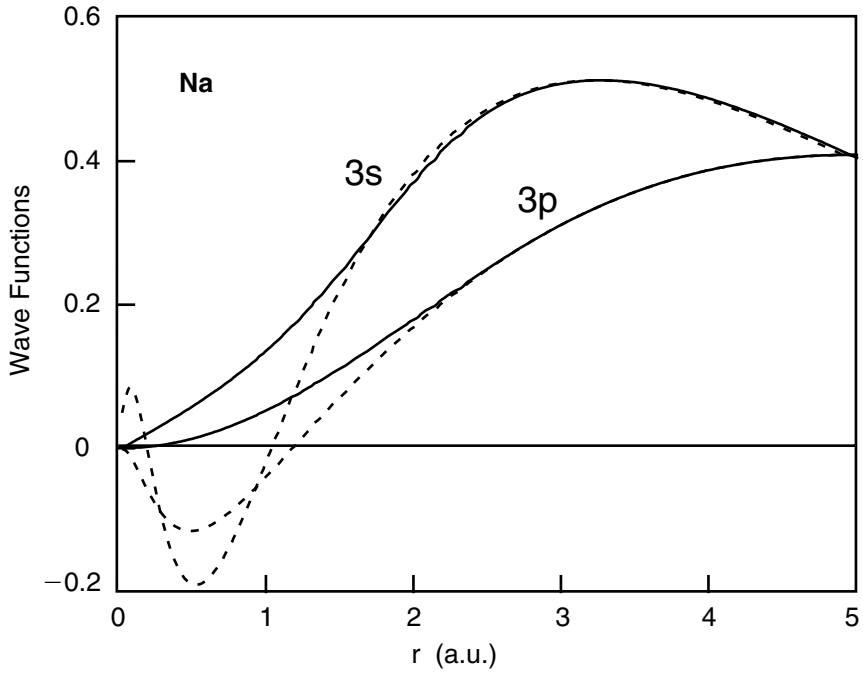

Figure 2. Pseudopotential wave functions compared to all-electron wave functions for the sodium atom. The all-electron wave functions are indicated by the dashed lines.

Since the pseudopotential and corresponding wave functions vary slowly in space, a number of simple basis sets is possible, e.g., one could use Gaussians [9] or plane waves [6, 7]. Both methods often work quite well, although each has its limitations. Owing in part to the simplicity and ease of implementation, plane wave methods have become of the method of choice for electronic structure work, especially for simple metals and semiconductors like silicon [7, 10]. Methods based on plane wave bases are often called "momentum" or "reciprocal" space approaches to the electronic structure problem. Plane wave approaches utilize a basis of "infinite extent." The extended basis requires special techniques to describe localized systems. For example, suppose one wishes to examine a cluster of silicon atoms. A common approach is to use a "supercell method." The cluster would be placed in a large cell, which is periodically repeated to fill up all space. The electronic structure of this system corresponds to an isolated cluster, provided sufficient "vacuum" surrounds each cluster. This method is very successful and has been used to consider localized systems such as clusters as well as extended systems such as surfaces or liquids [10].

In contrast, one can take a rather dramatic alternative view and eliminate an explicit basis altogether and solve Eq. (6) completely in *real space* using

a grid. Real space or grid methods are typically used for engineering problems, e.g., one might solve for the strain field in an airplane wing using finite element methods. Such methods have not been commonly used for the electronic structure problem. There are at least two reasons for this situation. First, without the pseudopotential method, a nonlinear grid would be needed to describe the singular coulombic potential near the atomic nucleus and the corresponding cusp in the wave function. This would enormously complicate the problem and destroy the simplicity of the method. Second, the non-local nature of the pseudopotential can be easily addressed in grid methods, but until recently the formalism for this task has not been available.

Real-space approaches overcome many of the complications involved with explicit basis, especially for describing nonperiodic systems such as molecules, clusters and quantum dots. Unlike localized orbitals such as Gaussians, the basis is unbiased. One need not specify whether the basis contains particular angular momentum components. Moreover, the basis is not "attached" to the atomic positions and no Pulay forces need to be considered [11]. Pulay forces arise from an incomplete basis. As atoms are moved, the basis needs to be recomputed as the convergence changes with the atomic configuration. Unlike an extended basis such as those based on plane waves, the vacuum is easily described by grid points. In contrast to plane waves, grids are efficient and easy to implement on parallel platforms. Real space algorithms avoid the use of fast Fourier transforms by performing all calculations in physical space instead of Fourier space. A benefit of avoiding Fourier transforms is that very few global communications are required.

Different numerical methods can be used to implement real space methods such as finite element or finite difference methods. Both approaches have advantages and liabilities. Finite element methods can easily accommodate nonuniform grids and can reflect the variational principle as the mesh is refined [1]. This is an appropriate approach for systems in which complex boundary conditions exist. For systems where the boundary conditions are simple, e.g., outside a domain the wave function is set to zero, this is not an important consideration. Finite differencing methods are easier to implement compared to finite element methods, especially with uniform grids. Both approaches have been extensively utilized; however, owing to the ease of implementation, finite differencing methods have been applied to a wider range of materials and properties. For this reason, we will illustrate the finite differencing method.

A key aspect to the success of the finite difference method is the availability of *higher order finite difference expansions* for the kinetic energy operator, i.e., expansions of the Laplacian [12]. Higher order finite difference methods significantly improve convergence of the eigenvalue problem when compared with standard finite difference methods. If one imposes a simple, uniform grid

on our system where the points are described in a finite domain by (x_i, y_j, z_k), one may approximate the Laplacian operator at (x_i, y_j, z_k) by

$$\frac{\partial^2 \psi}{\partial x^2} = \sum_{n=-M}^{M} C_n \psi(x_i + nh, y_j, z_k) + O(h^{2M+2}), \tag{8}$$

where h is the grid spacing and M is a positive integer. This approximation is accurate to $\mathrm{O(h^{2M+2})}$ under the assumption that ψ can be approximated accurately by a power series in h. Algorithms are available to compute the coefficients C_n for arbitrary order in h [12].

With the kinetic energy operator expanded as in Eq. (8), one can set up the Kohn–Sham equation over a grid. For simplicity, let us assume a uniform grid, but this is not a necessary requirement. $\psi(x_i, y_j, z_k)$ is computed on the grid by solving the eigenvalue problem:

$$\begin{aligned} -\frac{\hbar^2}{2m} \Bigg[& \sum_{n_1=-M}^{M} C_{n_1} \psi_n(x_i + n_1 h, y_j, z_k) + \sum_{n_2=-M}^{M} C_{n_2} \psi_n(x_i, y_j + n_2 h, z_k) \\ & + \sum_{n_3=-M}^{M} C_{n_3} \psi_n(x_i, y_j, z_k + n_3 h) \Bigg] + \big[V_{\mathrm{ion}}(x_i, y_j, z_k) + V_{\mathrm{H}}(x_i, y_j, z_k) \\ & + V_{\mathrm{xc}}(x_i, y_j, z_k) \big] \psi_n(x_i, y_j, z_k) = E_n \psi_n(x_i, y_j, z_k) \end{aligned} \tag{9}$$

For L grid points, the size of the full matrix is L^2.

A uniformly spaced grid in a three-dimensional cube is shown in Fig. 3. Each grid point corresponds to a row in the matrix. However, many points in the cube are far from any atoms in the system and the wave function on these points may be replaced by zero. Special data structures may be used to discard these points and retain only those having a nonzero value for the wave function. The size of the Hamiltonian matrix is usually reduced by a factor of two to three with this strategy, which is quite important considering the large number of eigenvectors which must be saved. Further, since the Laplacian can be represented by a simple stencil, and since all local potentials sum up to a simple diagonal matrix, the Hamiltonian need not be stored.

Nonlocality in the pseudopotential, i.e., the "state dependence" of the potential as illustrated in Fig. 1, is easily treated using a plane wave basis in Fourier space, but it may also be calculated in real space. The nonlocality appears only in the angular dependence of the potential and not in the radial coordinate. It is often advantageous to use a more advanced projection scheme, due to Kleinman and Bylander [13]. The interactions between valence electrons and pseudo-ionic cores in the Kleinman–Bylander form may be separated into a local potential and a nonlocal pseudopotential in *real space* [8], which differs from zero only inside the small core region around each atom.

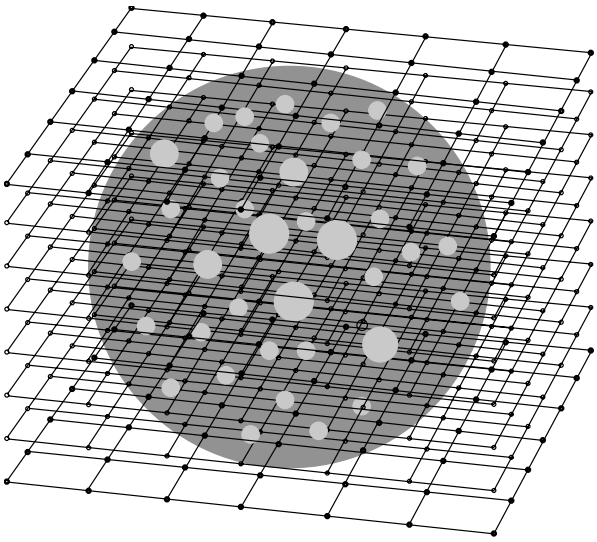

Figure 3. Uniform grid illustrating a typical configuration for examining the electronic structure of a localized system. The gray sphere represents the domain where the wave functions are allowed to be nonzero. The light spheres within the domain are atoms.

One can write the Kleinman–Bylander form in real space as

$$V_{\text{ion}}^{\text{p}}(\vec{r})\phi_n(\vec{r}) = \sum_a V_{\text{loc}}(|\vec{r}_a|)\phi_n(\vec{r}) + \sum_{a,\ n,lm} G_{n,lm}^a u_{lm}(\vec{r}_a)\,\Delta V_l(r_a), \tag{10}$$

$$K_{n,lm}^a = \frac{1}{\langle \Delta V_{lm}^a \rangle} \int u_{lm}(\vec{r}_a)\,\Delta V_l(r_a)\,\psi_n(\vec{r})\mathrm{d}^3 r, \tag{11}$$

and $\langle \Delta V_{lm}^a \rangle$ is the normalization factor,

$$< \Delta V_{lm}^a > = \int u_{lm}(\vec{r}_a)\,\Delta V_l(r_a) u_{lm}(\vec{r}_a)\,\mathrm{d}^3 r, \tag{12}$$

where $\vec{r}_a = \vec{r} - \vec{R}_a$, and the u_{lm} are the atomic pseudopotential wave functions of angular momentum quantum numbers (l, m) from which the l-dependent ionic pseudopotential, $V_l(r)$, is generated. $\Delta V_l(r) = V_l(r) - V_{\text{loc}}(r)$ is the difference between the l component of the ionic pseudopotential and the local ionic potential.

As a specific example, in the case of Na, we might choose the local part of the potential to replicate only the $l = 0$ component as defined by the 3s state. The nonlocal parts of the potential would then contain only the $l = 1$ and $l = 2$ components. The choice of which angular component is chosen for the local part of the potential is somewhat arbitrary. It is often convenient to chose the local potential to correspond to the highest l-component of interest. This

reduces the computational effort associated with higher l-components [3]. The choice of the local potential can be tested by utilizing different components for the local potential.

There are several difficulties with the eigen problems generated in this application in addition to the size of the matrices. First, the number of required eigenvectors is proportional to the atoms in the system, and can grow up to thousands. Besides storage, maintaining the orthogonality of these vectors can be a formidable task. Second, the relative separation of the eigenvalues becomes increasingly poor as the matrix size increases and this has an adverse effect on the rate of convergence of the eigenvalue solvers. Preconditioning techniques attempt to alleviate this problem. A brief review of these approaches can be found in Ref. [3].

The architecture of the Hamiltonian matrix is illustrated in Fig. 4 for a diatomic molecule. Although the details of matrix structure will be a function of the geometry of the system, the essential elements remain the same. The off-diagonal elements arise from the expansion coefficients in Eq. (8) and the nonlocal potential in Eq. (10). These elements are not updated during the self-consistency cycle. The on-diagonal matrix elements consist of the local ion core pseudopotential, the Hartree potential and the exchange-correlation potential. These terms are updated each self-consistent cycle.

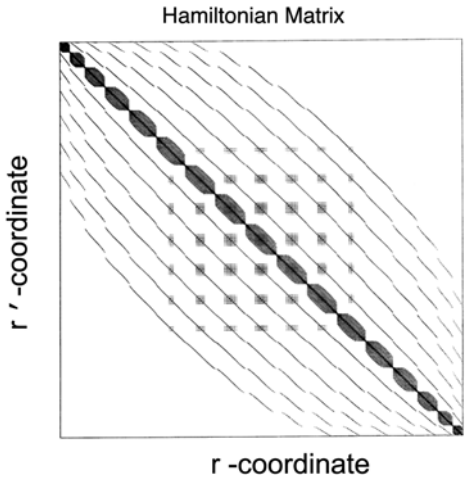

Figure 4. Hamiltonian matrix for a diatomic molecule in real space. Nonzero matrix elements are indicated by black dots. The diagonal matrix elements consist of the local ionic pseudopotential, Hartree potential and local density exchange-correlation potential. The off-diagonal matrix elements consistent of the coefficients in the finite difference expansion and the nonlocal matrix elements of the pseudopotential. The system contains about 4000 grid points or 16 million matrix elements.

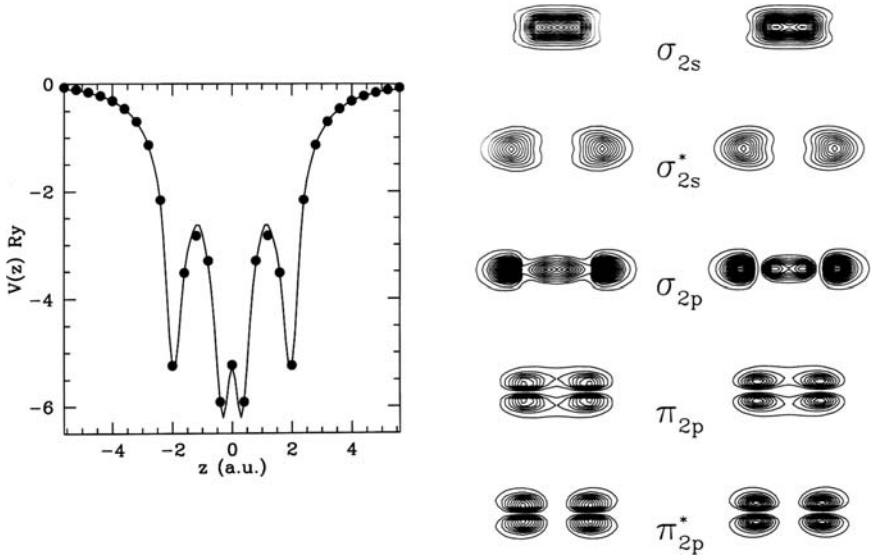

Figure 5. Potentials and wave functions for the oxygen dimer molecule. The total electronic potential is shown on the left along a ray connecting the two oxygen atoms. The Kohn–Sham molecular orbitals are shown on the right side of the figure. The orbitals on the left are from a real space calculation and the ones on the right from a plane wave calculation.

While the Hamiltonian matrix in real space can be large, it never needs to be explicitly saved. Also, the matrix is sparse; the sparsity is a function of M (see Eq. 8), which is the order of the higher order difference expansion. For larger values of M, the grid can be made coarse. However, this reduces the sparsity of the matrix. Conversely if we use standard finite difference methods, the matrix is sparser, but the grid size must be fine to retain the same accuracy. In practice, a value of $M = 4-6$ appears to work very well.

There is a close relationship between the plane wave method and real-space methods. For example, one can always do a Fourier transform on a real-space method and obtain results in reciprocal space, or perform the operation in reverse to go from Fourier space to real space. In this sense, higher order finite differences can be considered an abridged Fourier transform as one does not sum over all grid points in the mesh. As a rough measure of the convergence of real space methods, one can consider a Fourier component or plane wave cut off of $(\pi / h)^2$ for a grid spacing, h. Using this criterion, a grid spacing of $h = 0.5$ a.u.[1] would correspond to a plane wave cut-off of approximately 40 Ry.

In Fig. 5, a comparison is between the plane-wave supercell method and a real-space method for the oxygen dimer. The oxygen dimer is a difficult

[1] 1 a.u. = 0.529 Å or one bohr unit of length.

molecular species using pseudopotentials as the potential is rather deep and quite nonlocal as compared to second row elements such as silicon. The total local electronic potential is depicted along a ray containing the oxygen atoms [14]. Also shown are the Kohn–Sham one electron orbitals. The agreement between the two methods is quite good, certainly less than the uncertainties involved in the local density approximation. The most noticeable difference in the potential occurs at the nuclear positions. At this point, the atomic pseudopotential are quite strong and the variation in the wave function requires a fine mesh. However, it is important to note that this spatial regime is removed from the bonding region of the molecule. A survey of cluster and molecular species using both plane waves and real space method confirms that the accuracy of the two methods is comparable, but the real space method is easier to implement [14].

3. Outlook

The focus of the electronic structure problem will likely not reside in solving for the energy bands of ordered solids. The energy band structure of crystalline matter, especially elemental solids, has largely been exhausted. This is not to say that elemental solids are no longer of interest. Certainly, interest in these materials will continue as testing grounds for new electronic structure methods. However, interest in nonperiodic systems such as amorphous solids, liquids, glasses, clusters, and nanoscale quantum dots is now a major focus of the electronic structure problem. Perhaps this is the greatest challenge for electronic structure methods, i.e., systems with many electronic and nuclear degrees of freedom and little or no symmetry. Often the structure of these materials are unknown and the materials properties may be a strong function of temperature.

Real-space methods offer a new avenue for these large and complex systems. As an illustration of the potential of these methods, consider the example of quantum dots. In Fig. 6, we illustrate hydrogenated Ge clusters. These clusters are composed of bulk fragments of Ge whose dangling bonds are capped with hydrogen. The hydrogen passivates any electronically active dangling bonds. The larger clusters correspond to quantum dots, i.e., semiconductor fragments whose surface properties have been removed, but whose optical properties are dramatically altered by quantum confinement. It is well known that these systems have optical properties with much larger gaps than that of the bulk crystal. The optical spectra of such clusters are shown in Fig. 7. The largest cluster illustrated contains over 800 atoms, although even larger clusters have been examined. This size cluster would be difficult to examine with traditional methods. Although these calculations were done with a ground state method the general shape of the spectra are correct and the evolution of the

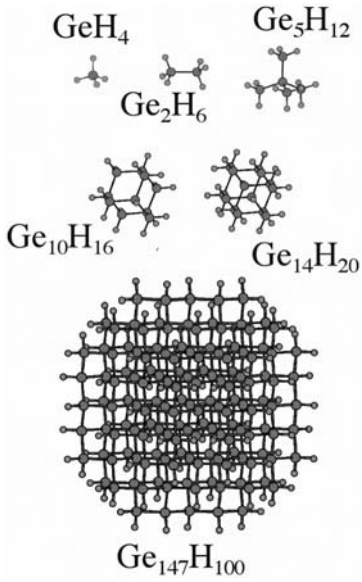

Figure 6. Hydrogenated germanium clusters ranging from germane (GeH_4) to $Ge_{147}H_{100}$.

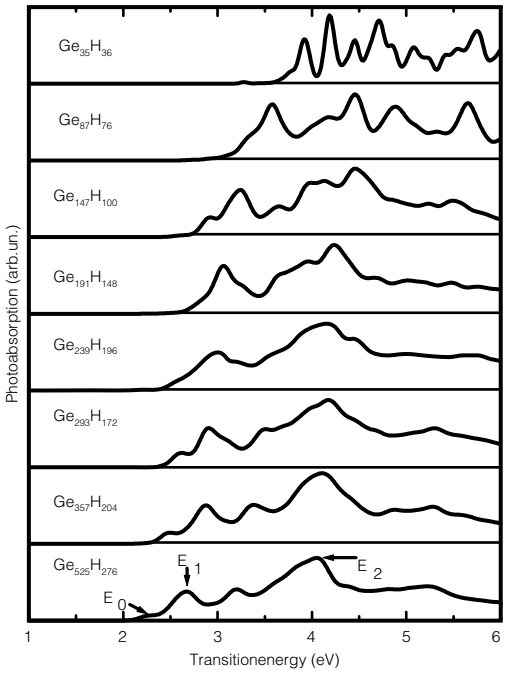

Figure 7. Photoabsorption spectra for hydrogenated germanium quantum dots. The labels E_0, E_1 and E_2 refer to optical features.

spectra appear bulk-like by a few hundred atoms. Surfaces, clusters, magnetic systems, complex solids have also been treated with real-space methods [1, 15].

Finally, systems approach the macroscopic limit, it is common to employ finite element or finite difference methods to describe material properties. One would like to couple these methods to those appropriate at the quantum (or nano) limit. The use of real space methods at these opposite limits would be a natural choice. Some attempts along these lines exist. For example, fracture methods often divide up a problem by treating the fracture tip with quantum mechanical methods, the surrounding area by molecular dynamics and the medium away from the tip by continuum mechanics [16].

References

[1] T.L. Beck, "Real-space mesh techniques in density functional theory," *Rev. Mod. Phys.*, 74, 1041, 2000.
[2] J.R. Chelikowsky, "The pseudopotential-density functional method applied to nanostructures," *J. Phys. D: Appl. Phys.*, 33, R33, 2000.
[3] C.L. Bris (ed.), *Handbook of Numerical Analysis (Devoted to Computational Chemistry)*, Volume X, Elsevier, Amsterdam, 2003.
[4] S. Lundqvist and N.H. March (eds.), *Theory of the Inhomogeneous Electron Gas*, Plenum, New York, 1983.
[5] W. Kohn and L.J. Sham, "Self-consistent equations including exchange and correlation effects," *Phys. Rev.,* 140, A1133, 1965.
[6] W. Pickett, "Pseudopotential methods in condensed matter applications," *Comput. Phys. Rep.*, 9, 115, 1989.
[7] J.R. Chelikowsky and M.L. Cohen, "*Ab initio* pseudopotentials for semiconductors," In: T.S. Moss and P.T. Landsberg (eds.), *Handbook of Semiconductors*, 2nd edn., Elsevier, Amsterdam, 1992.
[8] N. Troullier and J.L. Martins, "Efficient pseudopotentials for plane-wave calculations," *Phys. Rev. B*, 43, 1993, 1991.
[9] J.R. Chelikowsky and S.G. Louie, "First principles linear combination of atomic orbitals method for the cohesive and structural properties of solids: application to diamond," *Phys. Rev. B*, 29, 3470, 1984.
[10] J.R. Chelikowsky and S.G. Louie (eds.), *Quantum Theory of Materials*, Kluwer, Dordrecht, 1996.
[11] P. Pulay, "*Ab initio* calculation of force constants and equilibrium geometries," *Mol. Phys.*, 17, 197, 1969.
[12] B. Fornberg and D.M. Sloan, "A review of pseudospectral methods for solving partial differential equations," *Acta Numerica*, 94, 203, 1994.
[13] L. Kleinman and D.M. Bylander, "Efficacious form for model pseudopotential," *Phys. Rev. Lett.*, 48, 1425, 1982.
[14] J.R. Chelikowsky, N. Troullier, and Y. Saad, "The finite-difference-pseudopotential method: electronic structure calculations without a basis," *Phys. Rev. Lett.*, 72, 1240, 1994.

[15] J. Bernholc, "Computational materials science: the era of applied quantum mechanics," *Phys. Today*, 52, 30, 1999.

[16] A. Nakano, M.E. Bachlechner, R.K. Kalia, E. Lidorkis, P. Vashishta, G.Z. Voyladjis, T.J. Campbell, S. Ogata, and F. Shimojo, "Multiscale simulation of nanosystems," *Comput. Sci. Eng.*, 3, 56, 2001.